

Anomalous single top quark production at the THERA and Linac⊗LHC based γp colliders

O. Çakır^a, S. Sultansoy^{b,c}, M. Yılmaz^b

^a *Ankara University, Faculty of Sciences,
Department of Physics, 06100,
Tandogan, Ankara, Turkey.*

^b *Gazi University, Faculty of Arts and Sciences,
Department of Physics, 06500,
Besevler, Ankara, Turkey.*

^c *Institute of Physics, Academy of Sciences,
H. Cavid Avenue, 370143, Baku, Azerbaijan.*

Single production of t-quarks at the THERA and Linac⊗LHC based γp colliders via anomalous γut and γct couplings have been studied. We show that γp colliders will be a powerful tool for searching for the anomalous couplings.

Although the standard model (SM) has been proved to be phenomenologically successful at the available energies, there have been intensive studies to test the deviations from the SM at higher energy scales. Because of its large mass ($m_t \cong 175$ GeV), the top quark is believed to be more sensitive to new physics than other particles. Recently, the production of single t-quarks at LEP and HERA was studied in [1]. A possible anomalous γut and γct couplings are generated in a dynamical theory of mass generation. These anomalous vertices can be examined at future lepton and lepton-hadron colliders. An essential step in this direction will be provided by THERA [2] and Linac⊗LHC [3] based γp colliders (see also review [4]). The main parameters of these γp colliders are given in the Table I.

Although CDF [5] have shown that $t \rightarrow cg$ and $t \rightarrow c\gamma$ decays are not the most significant decay modes, high energy photon may provide anomalous single top production with the anomalous couplings accessible in the realistic ranges. In this note we study the potential of the γp colliders in search for single t quark production in the resonance channel via anomalous coupling.

The possible anomalous couplings of top quarks lead to the following effective lagrangian for the neutral current interactions between the fermions and the gauge bosons

$$L^{eff} = L^{SM} + L^A \quad (1)$$

$$L^A = \frac{g_e}{\Lambda} \bar{t} \sigma_{\mu\nu} (A_\gamma + B_\gamma \gamma_5) q F^{\mu\nu} + \frac{g_Z}{\Lambda} \bar{t} \sigma_{\mu\nu} (A_Z + B_Z \gamma_5) q Z^{\mu\nu} \\ + \frac{g_s}{\Lambda} \bar{t} \sigma_{\mu\nu} (A_g + B_g \gamma_5) \frac{\lambda^a}{2} q G_a^{\mu\nu} + h.c. \quad (2)$$

where $F^{\mu\nu}$, $Z^{\mu\nu}$, and $G^{\mu\nu}$ are the field strength tensors of the photon, Z boson and gluons, respectively; λ is the QCD structure constant; g_e , g_Z , and g_s are the electroweak, and strong coupling constants, respectively. Constants $A_{\gamma,Z,g}$ and $B_{\gamma,Z,g}$ are the parameters for the projection operators and anomalous couplings. Finally, Λ is the cutoff of the effective theory.

Feynman diagram for single production of t quarks at γp collisions is shown in Fig. 1. Anomalous interaction of the t quarks with the photon is given explicitly

$$L_\gamma^A = \frac{g_e}{\Lambda} \bar{t} \sigma_{\mu\nu} [(A_u^t + B_u^t \gamma_5) u + (A_c^t + B_c^t \gamma_5) c] F^{\mu\nu} + h.c. \quad (3)$$

In general, the vertex factor for the anomalous top quark couplings can be rewritten including all undetermined constants and the scale parameter Λ

$$\frac{i}{m_t} (f_1 + f_2 \gamma_5) \sigma^{\mu\nu} k_\nu \quad (4)$$

where

$$f_1 = g_e A_i \frac{m_t}{\Lambda}, \quad f_2 = g_e B_i \frac{m_t}{\Lambda} \quad (5)$$

Decay width for top quarks in the SM channel $t \rightarrow bW$ is well known

$$\Gamma(t \rightarrow qW) = \frac{g_W^2 |V_{tb}|^2}{64\pi} \frac{1}{m_W^2} m_t^3 \left(1 - \frac{m_W^2}{m_t^2}\right) \left(1 + \frac{m_W^2}{m_t^2} - 2\frac{m_W^4}{m_t^4}\right) \quad (6)$$

which is dominant in the full decay mode. The total decay width may be enhanced by the anomalous decays. In this case the total decay widths will be the sum of all possible decay contributions

$$\Gamma(t \rightarrow qg) = \frac{g_s^2 C_F}{8\pi} \frac{1}{\Lambda^2} (|A_g|^2 + |B_g|^2) m_t^3 \quad (7)$$

$$\Gamma(t \rightarrow q\gamma) = \frac{g_e^2}{8\pi} \frac{1}{\Lambda^2} (|A_\gamma|^2 + |B_\gamma|^2) m_t^3 \quad (8)$$

$$\Gamma(t \rightarrow qZ) = \frac{g_Z^2}{8\pi} \frac{1}{\Lambda^2} (|A_Z|^2 + |B_Z|^2) m_t^3 \left(1 - \frac{m_Z^2}{m_t^2}\right) \left(1 - \frac{m_Z^2}{2m_t^2} - \frac{m_Z^4}{2m_t^4}\right) \quad (9)$$

where C_F is the color factor 4/3. Here, neglecting the terms $(m_{W,Z}/m_t)^2 < 1$, we estimate the ratio of the partial widths in the various channels $V = \gamma, Z, g$:

$$R_V = \frac{\Gamma(t \rightarrow qV)}{\Gamma(t \rightarrow bW)} \approx \frac{8g_V^2 (|A_V|^2 + |B_V|^2) m_W^2}{g_W^2 \Lambda^2 |V_{tb}|^2} \quad (10)$$

If we assume that all the constants A_V and B_V are of the same order, then the branchings are simply proportional to the gauge couplings g_V

$$g_s \approx 1.12, g_e \approx 0.31, g_W \approx 0.64 \text{ and } g_Z \approx 0.74 \text{ at } q^2 = m_Z^2 \quad (11)$$

where the dominant channel will be the gluon mediated anomalous interaction. Experimental limits for the anomalous decay channels of top quarks are given in [6]:

$$R_\gamma(t \rightarrow q\gamma) < 0.032 \quad \text{and} \quad R_Z(t \rightarrow qZ) < 0.33 \quad (12)$$

and the CDF data [5] for branching ratio of top quark decaying to bottom quark places the limit on the anomalous decay

$$BR(t \rightarrow qg) < 0.45 \quad (13)$$

We present the ratio of the partial widths for the top quark anomalous photonic decay vs. anomalous coupling parameter f in Fig. 2. In the same Figure, corresponding experimental bound is also given. One can see that SM channel ($t \rightarrow bW$) is dominant for realistic values of anomalous coupling $f < 0.06$.

The differential cross section for the resonant production of top quarks via the subprocess $\gamma q \rightarrow t \rightarrow Wb$ is

$$\begin{aligned} \frac{d\hat{\sigma}}{d\hat{t}} = & \frac{g_W^2 |V_{tb}|^2}{64\pi} \left[\frac{(A-B)^2 [m_t^2 (2m_W^4 + \hat{s}\hat{t} - 2m_W^2(\hat{s} + \hat{t}))]}{m_t^2 m_W^2 \hat{s} [(\hat{s} - m_t^2)^2 + m_t^2 \Gamma_t^2]} \right. \\ & \left. - \frac{[\hat{s}^2(\hat{s} + \hat{t}) - m_W^2 \hat{s}(\hat{s} + 2\hat{t})] (A+B)^2}{m_t^2 m_W^2 \hat{s} [(\hat{s} - m_t^2)^2 + m_t^2 \Gamma_t^2]} \right] \quad (14) \end{aligned}$$

corresponding cross section is given by

$$\begin{aligned} \hat{\sigma}(\gamma q \rightarrow t \rightarrow Wb) = & \frac{g_W^2 |V_{tb}|^2}{128\pi} \frac{(\hat{s} - m_W^2)^2 (\hat{s} + 2m_W^2)}{m_t^2 m_W^2} \\ & \times \frac{[(A^2 + B^2)(\hat{s} + m_t^2) - 2AB(\hat{s} - m_t^2)]}{\hat{s} [(\hat{s} - m_t^2)^2 + m_t^2 \Gamma_t^2]} \quad (15) \end{aligned}$$

In order to see how the anomalous coupling parameters f_i change the transverse momentum distributions of the quark-jet, we derive the following formula ($V = W, Z, \gamma$)

$$\begin{aligned} \frac{d\sigma}{dp_T}(\gamma p \rightarrow V + jet) &= 2p_T \int_{y_{\min}}^{y_{\max}} dy \int_{x_a^{\min}}^{0.83} dx_a f_{\gamma/e}(x_a) f_{q/p}(x_b, Q_p^2) \\ &\times \frac{x_a x_b s}{x_a s - 2m_T E_p e^y} \frac{d\hat{\sigma}}{d\hat{t}}(\hat{s}, \hat{t}, f_i) \end{aligned} \quad (16)$$

where

$$y_{\min}^{(\max)} = \log \left[x \pm \sqrt{x^2 - 0.83 E_e / E_p} \right] \quad (17)$$

$$x = \frac{0.83s + m_q^2 - m_V^2}{4m_T E_p}, \quad m_T = m_q^2 + p_T^2 \quad (18)$$

$$x_a^{\min} = \max(x_a^{(1)}, x_a^{(2)}) \quad (19)$$

$$x_a^{(1)} = \frac{2m_T E_p e^y - m_q^2 + m_V^2}{s - 2m_T E_e e^{-y}}, \quad x_a^{(2)} = \frac{(m_q + m_V)^2}{s} \quad (20)$$

$$x_b = \frac{2m_T E_e x_a e^{-y} - m_q^2 + m_V^2}{x_a s - 2m_T E_p e^y} \quad (21)$$

with the Mandelstam variables

$$\hat{s} = x_a x_b s, \quad \hat{t} = m_q^2 - 2E_e x_a m_T e^{-y} \quad (22)$$

For the numerical calculation, we have used the quark distributions $f_{q/p}(x_b, Q_p^2)$ [7] in the proton and the Compton backscattered high energy photon spectrum $f_{\gamma/e}(x_a)$ [8]

$$f_{\gamma/e}(x) = \begin{cases} N \left[1 - x + \frac{1}{1-x} \left[1 - \frac{4x}{x_0} \left(1 - \frac{x}{x_0(1-x)} \right) \right] \right], & 0 < x < x_{\max} \\ 0, & x > x_{\max} \end{cases} \quad (23)$$

where $x_0 = 4.82$, $x_{\max} = x_0/(1+x_0)$, $N = 1/1.84$. The p_T distributions of the b-jet in the final state for THERA 1,2 and 3 options, and Linac⊗LHC are shown in Figures 3-5.

The differential cross sections for the signal processes $\gamma u \rightarrow t \rightarrow Wb$ and $\gamma c \rightarrow t \rightarrow Wb$ via transverse momentum of the b -jet are peaked around the value

$$p_T^b = \sqrt{\left[\frac{m_t^2 - m_W^2 + m_b^2}{2m_t} \right]^2 - m_b^2} \approx 69 \text{ GeV} \quad (24)$$

whereas the backgrounds contribute mainly ($\sim 2 \times 10^{-4}$ pb/GeV) at low p_T . The cross sections for higher values of the anomalous couplings show up over the background continuum.

In the case of the Option 1(or 2) of the THERA, about the 70% of the signal cross section ($\Delta\sigma^S \sim 12.4$ fb at $f = 10^{-3}$) lies in the p_T window 50 – 70 GeV. Whereas the background cross section in this interval is only $\Delta\sigma^B \sim 0.9$ fb. Therefore, high p_T cut in this interval could help to eliminate background from the signal. The values of the cross sections for both signal and backgrounds for different f can be found in Table II. Here, the differential cross sections are integrated over a chosen p_T window (50-70 GeV) in order to find the statistical significance $S/\sqrt{S+B}$ (here S stands for signal and B for background). From the Table II, one can see that anomalous couplings down to 10^{-3} can be reached at THERA based γp collider. This value could be 10^{-4} at Linac⊗LHC based γp collider. We have used the integrated luminosity for the THERA options as $L_1^{int} = 120\text{pb}^{-1}$, $L_2^{int} = 750\text{pb}^{-1}$, $L_3^{int} = 480\text{pb}^{-1}$ and the luminosity $L^{int} = 3 \times 10^4\text{pb}^{-1}$ for Linac⊗LHC based γp collider.

Let us estimate the total cross section for the signal process $\gamma p \rightarrow WbX$, via the resonant production of top quark. The signal and background total cross sections can be written as

$$\sigma(\gamma p \rightarrow WbX) = \int_{\tau_{\min}}^{0.83} d\tau \int_{\tau/0.83}^1 \frac{dx}{x} f_{\gamma/e}(\tau/x) f_{q/p}(x, Q_p^2) \hat{\sigma}(\tau s, f_i) \quad (25)$$

The total cross sections for the single top production $\gamma p \rightarrow t \rightarrow Wb$ depending on the coupling f and the background $\gamma p \rightarrow Wb$ using laser and WW photon spectrum at THERA and Linac \otimes LHC based γp colliders are shown in Figures 6 and 7.

In Eq. (25), $f_{\gamma/e}(y)$ is the function which describes the spectrum of photons scattered backward from the interaction of laser light with the high energy electron beam (23) or the Weizsaecker-Williams (WW) approximated photon spectrum [9]

$$f_{\gamma/e}(y) = \frac{\alpha}{2\pi} \log \left[\frac{(1-y)}{y^2 \delta} \left(\frac{1+(1-y)^2}{y} \right) - \frac{2(1-y-\delta y^2)}{y} \right] \quad (26)$$

where α is the fine structure constant, $\delta = (m/Q_{\max})^2$, Q_{\max} being the photon virtuality region, and m is the mass of incoming particle. It should be noted that the total cross sections with Compton bacscattered photons are about ten times larger than the corresponding cross sections with the WW photons. This makes the γp colliders powerful machines in searching for the new physics. The total number of signal events are given in Table III.

In conclusion, top quark can be produced at γp colliders in the resonance channel via anomalous interaction. The main decay mode for t quarks is the $b + W$. For this channel b quarks can be identified in the detector as b -jets (so called b -tagging), the hadronic decay modes of W -boson will be identified as two-jets and its leptonic decay as a lepton+missing p_T . The b -quarks from the decay of top quarks have higher transverse momentum than those from the backgrounds. This makes the signal separable from the backgrounds even at small f . As can be seen from the Tables II and III, we can observe the anomalous interactions for t quarks down to the couplings $f = 2 \times 10^{-3}$ for THERA and $f = 2 \times 10^{-4}$ for Linac \otimes LHC based γp colliders within the statistical acceptance.

- [1] H. Fritzsch, D. Holtmannspötter, Phys. Lett. B457, (1999) 186-192.
- [2] H. Abramowicz *et al.*, THERA Collaboration, in TESLA TDR, to be published (2001); A.K. Çiftçi, S. Sultansoy and Ö. Yavaş, EPAC 2000, p388 (2000).
- [3] A.K. Çiftçi *et al.*, Nucl. Instr. Meth. A365 (1995) 317; A.K.Çiftçi, S. Sultansoy and Ö. Yavaş, Proc. of EPAC 2000, p391 (2000).
- [4] S. Sultansoy, DESY Preprint, 99-159 (1999).
- [5] J. Incandela, (CDF Collaboration), FERMILAB-CONF-95-237-E (1995).
- [6] D.E. Groom *et al.*, The European Physical Journal C15, 1 (2000).
- [7] A.D. Martin, R.G. Roberts, W.J. Stirling and R.S Thorne, Univ. Durham preprint DTP/98/10 (1998), [hep-ph/9803445], Eur. Phys. J. C4 (1998) 463.
- [8] I.F. Ginzburg *et al.*, Nucl. Instrum. Methods, 205 (1983) 47; 219 (1984) 5.
- [9] V.M. Budnev *et al.*, Phys. Rep. C15 (1975) 181; S. Frixione *et al.*, Phys. Lett. B319 (1993) 339.

TABLE I. Main parameters of the THERA and Linac⊗LHC based γp colliders

Machine	$E_e(\text{GeV})$	$E_p(\text{GeV})$	$\sqrt{s_{\gamma p}^{\text{max}}}(\text{GeV})$	$L_{\gamma p}(\text{cm}^{-2}\text{s}^{-1})$
1	250	1000	911	4×10^{30}
THERA 2	500	500	911	2.5×10^{31}
3	800	800	1456	1.6×10^{31}
Linac⊗LHC	1000	7000	4820	1×10^{33}

 TABLE II. Cross sections in the chosen p_T window (50-70 GeV) and statistical significance for single top quark production at the THERA and Linac⊗LHC based γp colliders. S and B stand for the number of events for signal and background, respectively.

Machine ↓	$f \rightarrow$	10^{-1}	10^{-2}	10^{-3}	10^{-4}
THERA 1	$\Delta\sigma^S(\text{pb})$	7.94×10^1	1.24×10^0	1.24×10^{-2}	1.24×10^{-4}
	$S/\sqrt{S+B}$	9.76×10^1	1.22×10^1	1.18×10^0	4.28×10^{-2}
THERA 2	$\Delta\sigma^S(\text{pb})$	7.94×10^1	1.24×10^0	1.24×10^{-2}	1.24×10^{-4}
	$S/\sqrt{S+B}$	2.44×10^2	3.05×10^1	2.95×10^0	1.07×10^{-1}
THERA 3	$\Delta\sigma^S(\text{pb})$	4.27×10^1	6.66×10^{-1}	6.69×10^{-3}	6.69×10^{-5}
	$S/\sqrt{S+B}$	1.43×10^2	1.78×10^1	1.52×10^0	2.82×10^{-2}
Linac⊗LHC	$\Delta\sigma^S(\text{pb})$	1.56×10^2	2.43×10^0	2.44×10^{-2}	2.45×10^{-4}
	$S/\sqrt{S+B}$	2.16×10^3	2.69×10^2	2.06×10^1	3.15×10^{-1}

 TABLE III. Total cross sections and number of events for single top quark production. N_i are the number of signal events for the integrated luminosities given in the text.

$f \rightarrow$	10^{-1}	10^{-2}	10^{-3}	10^{-4}
$\sigma_{1,2}(\text{pb})$	1.13×10^2	1.27×10^0	1.27×10^{-2}	1.27×10^{-4}
N_1	1.36×10^4	1.52×10^2	1.52×10^0	1.52×10^{-2}
N_2	8.48×10^4	9.53×10^2	9.53×10^0	9.53×10^{-2}
$\sigma_3(\text{pb})$	7.87×10^1	7.99×10^{-1}	7.99×10^{-3}	7.99×10^{-5}
N_3	3.78×10^4	3.83×10^2	3.84×10^0	3.83×10^{-2}
$\sigma_{\text{LHC}}(\text{pb})$	2.31×10^2	2.31×10^0	2.31×10^{-2}	2.31×10^{-4}
N_{LHC}	6.93×10^6	6.93×10^4	6.93×10^2	6.93×10^0

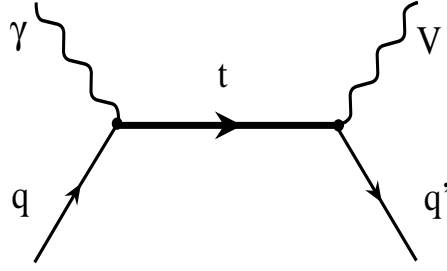


FIG. 1. Feynman diagram for single t production. Here q denotes the quarks u or c ; V stands for the gauge bosons (γ, Z, g, W).

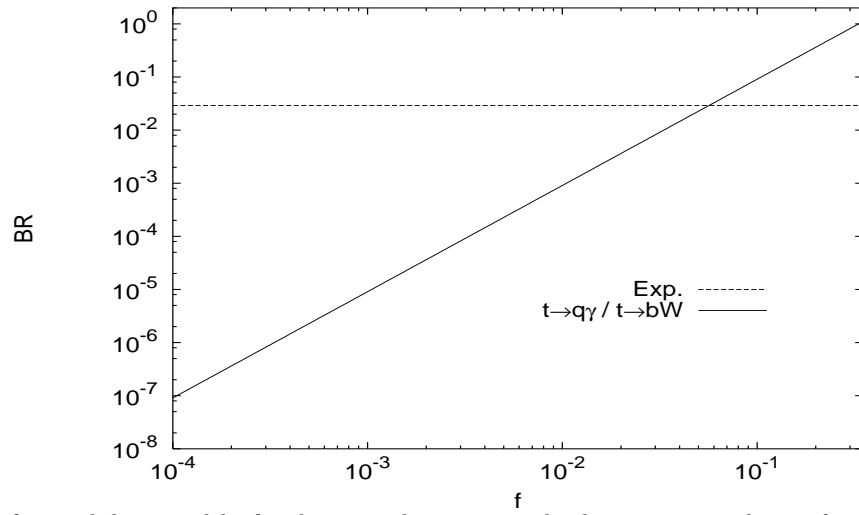


FIG. 2. The ratio of partial decay widths for the anomalous top quark, the experimental ratio for this channel is also given, $f = |f_1| = |f_2|$.

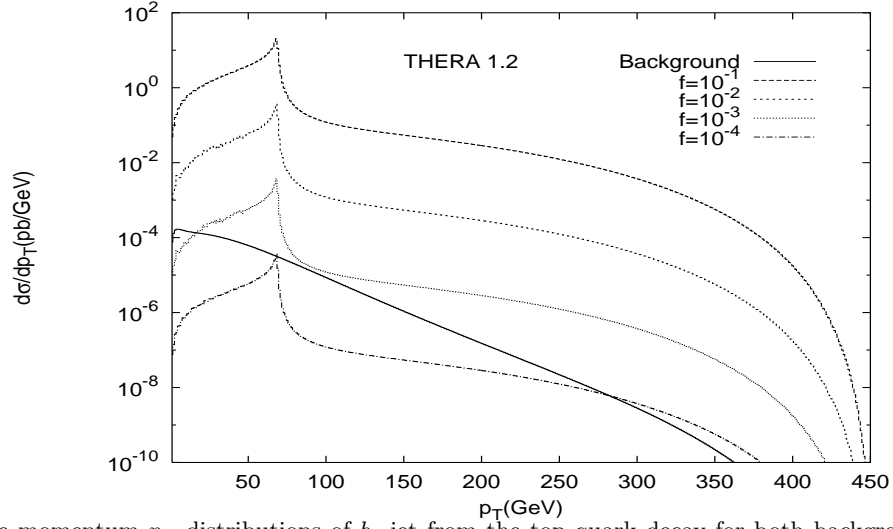


FIG. 3. Transverse momentum p_T distributions of b -jet from the top quark decay for both background and the signal at $f = 0.1, 0.01, 0.001$ and 0.0001 .

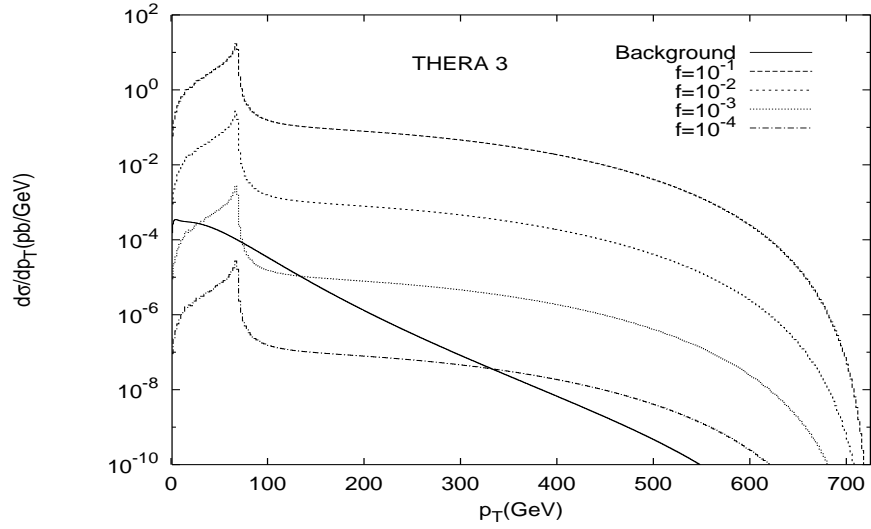


FIG. 4. The same as Figure 3 for THERA 3 option.

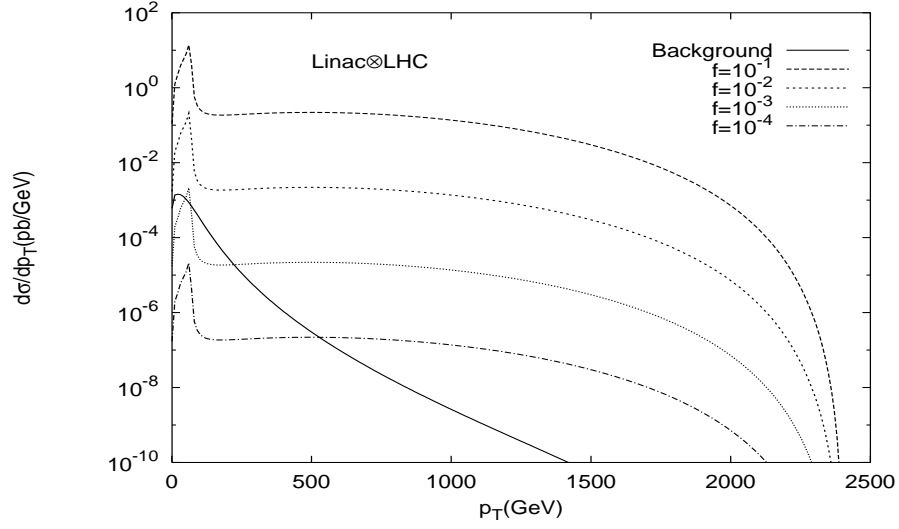


FIG. 5. The same as Figure 3 for Linac⊗LHC based γp collider.

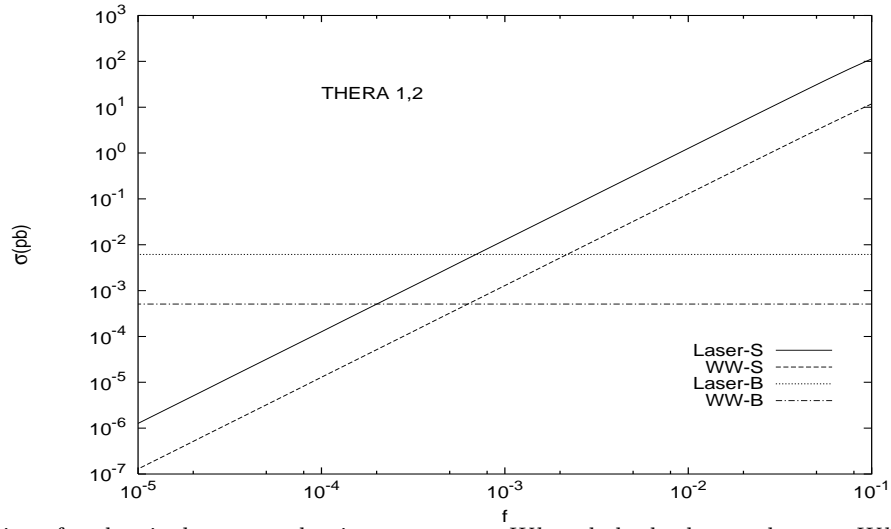


FIG. 6. Cross sections for the single top production $\gamma p \rightarrow t \rightarrow Wb$ and the background $\gamma p \rightarrow Wb$ using laser and WW photon spectrum depending on the coupling f at THERA 1 and 2 based γp colliders.

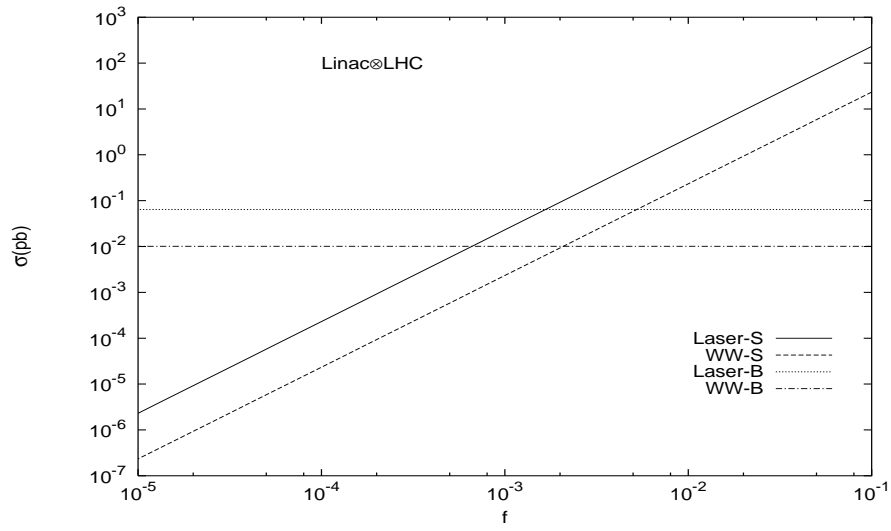


FIG. 7. The same as Figure 6 for Linac-LHC based γp collider.